EurJIC
European Journal of Inorganic Chemistry
Research Article
doi.org/10.1002/ejic.202400237
Chemistry Europe
European Chemical Societies Publishing
www.eurjic.org

Ionic-Liquid-Supported Magnetic Nanoparticles: Synthesis, Characterization, and Their Use for the Separation of Co and Ni from Li in Aqueous Solutions

Joana C. Almeida,[a, b] Celso E. D. Cardoso,[a, b] Márcia Neves,[a] Tito Trindade,[a] Mara G. Freire,[a] and Eduarda Pereira*[b]

The evolution of the electric vehicle market and the ongoing demand for lithium (Li), cobalt (Co) and nickel (Ni) for batteries production requires secondary sources for obtaining these elements. The recycling of Li-ion batteries involves hydrometallurgical processes with potential environmental implications, hence there is an urgent need for sustainable and more efficient recycling methods. Functionalized colloidal magnetic nanomaterials have gained interest as sorbents as they can selectively bind and remove metal species from waters, allowing their easy recovery through magnetic separation. This work addresses the preparation and evaluation of silica-coated magnetite nanoparticles (NPs), as alternative materials to recover Co and Ni from aqueous media, after their surface modification with 1-methyl-3-propylimidazolium chloride. The magnetic nanosorbents were fully characterized and the influence of solution pH and amount of ILs on the NPs surface was evaluated. Our research allows us to conclude that IL functionalized magnetic nanoparticles can be explored as an alternative to hydrometallurgical processes for the separation of Co and Ni from alkaline lixiviates of spent lithium-ion battery (LIB) powders.

Introduction

The production of electric vehicles has increased during the last years. This increase is imperative to decrease carbon emissions following investments made for advancing battery technology to enhance its energy efficiency. This tendency should keep growing as governments implement policies to encourage the transition to electric vehicles and battery technology becomes more accessible.[1]

Lithium (Li), cobalt (Co) and nickel (Ni) are metals commonly used to produce batteries of electric vehicles. Despite Li being found in lake brines and the other metals in natural ores, their extraction not only causes environmental concerns, but is also an expensive and inefficient process in terms of energy and resources.[2,3]

As the demand for these elements continues to rise due to battery production, the recovery of Li, Co and Ni from secondary sources, such as spent Li-ion batteries, will contribute for promoting environmental sustainability. Moreover, this strategy decreases the amount of hazardous wastes generated by improperly disposing of used batteries. Currently, the recovery of these metals from secondary sources involves hydrometallurgical processes in the leaching of spent Li-ion batteries and subsequent separation of Li, Co and Ni.[4] Since hydrometallurgical processes require volatile organic solvents and hazardous chemicals, the development of cost-efficient techniques able to separate lithium, cobalt and nickel from aqueous solutions is an urgent need of modern society.

Functionalized colloidal magnetic nanoparticles have received attention for magnetic separation-assisted adsorption technologies.[5,6] Among magnetic materials, magnetite nanoparticles stand out due to their unique properties, including high magnetic responsiveness and stability. Furthermore, they have the ability for surface functionalization aiming at the capture of target pollutants.[7,8] To this end, surface functionalization using ionic liquids (ILs) can be seen as a promising and alternative strategy for applying magnetic nanosorbents to capture target species, namely in scenarios in which other systems are not effective. Among the advantages of ILs, their high performance for metals extraction stands out, which can be achieved by selection of the IL chemical structure. Additionally, IL are chemically and thermally stable, further increasing the interest in this applied context.[9,10]

The extraction of lithium has been previously addressed using ILs based on ammonium and phosphonium cations from acidic aqueous solutions, showing efficiencies superior to 80%. Cobalt and nickel have also been extracted from chloride solutions using ILs.[11] In these processes, the sorption of these metals relies on the formation of metal chloride complexes, specifically lithium chloride (LiCl), cobalt chloride ($[CoCl_4]^{2-}$), and nickel chloride (predominant $Ni(H_2O)_5Cl]^+$).[12] Subsequently, ion pairs are formed between the chloride complexes and the IL, facilitating the extraction of these metal cations. Importantly, the selectivity of extraction for different metal ions can be controlled by their differences in complex behavior when using different types of ionic liquids.[12] For example, Schaeffer et al.[13] recognized the importance of separating the transition metals,

[a] *J. C. Almeida, C. E. D. Cardoso, M. Neves, T. Trindade, M. G. Freire*
Chemistry Department and CICECO-Aveiro Institute of Materials, University of Aveiro, Campus de Santiago, 3810-193 Aveiro, Portugal

[b] *J. C. Almeida, C. E. D. Cardoso, E. Pereira*
Chemistry Department and LAQV-REQUIMTE, University of Aveiro, Campus de Santiago, 3810-193 Aveiro, Portugal
E-mail: eduper@ua.pt

Supporting information for this article is available on the WWW under https://doi.org/10.1002/ejic.202400237

Research Article
doi.org/10.1002/ejic.202400237

nickel, cobalt, and manganese from spent batteries and obtained the separation of Ni^{2+} and Co^{2+} through the exploration of the different intrinsic properties of these metals using $[P_{44414}]Cl$. The same behavior has been observed in the extraction of these metals from spent lithium-ion batteries using the ionic liquid $[P_{8888}]$[Oleate], as reported by Othman et al.[14] In their study, the extraction efficiency of Co^{2+} reached 99% using 8 M HCl (pH ≈ -0.9), followed by Ni^{2+} extraction after increasing the pH to approximately 1.

ILs hold great promise for the extraction and sorption of metal species from leaching solutions. However, practical limitations are associated with certain ILs, including low diffusion coefficients, high viscosity, and challenges related to product purification and solvent recycling.[15] To overcome these limitations, supported ILs (SILs) offer an alternative approach. SILs combine the benefits of a solid substrate with the tailored properties of ILs. Notably, SILs have been used as sorbents for the recovery of lithium, cobalt and nickel, by using diverse types of materials, which include membranes,[16–19] polymers[20] and silica-gel.[21,22] To the best of our knowledge, the development of IL functionalized magnetic NPs have not been reported in the selective uptake of metal species dissolved in aqueous solutions containing the above metal cations.

In this study, we demonstrate that the IL-supported magnetic nanoparticles used as sorbent materials facilitate the separation of cobalt and nickel from lithium, when present as mixtures in using aqueous solutions. The IL-supported magnetic nanoparticles, with different amounts of cation and anion, were prepared by covalently attaching the IL cation to the surface of silica-coated magnetite NPs. Imidazolium and chloride were investigated as the cation and counter-ion, respectively. The prepared NPs were chemically and morphologically characterized. The influence of the solution pH and the bonding amount of ILs on the NPs surface to separate Ni^{2+} and Co^{2+} from Li^{+} in aqueous media was evaluated.

Experimental Section

Materials

Chemicals were supplied by commercial sources and used without further purification: (3-chloropropyl)trimethoxysilane (>98%, Acros Organics), ammonium hydroxide solution (NH_3 in H_2O, 25%, Riedel-de-Häen), cobalt (Co^{2+} in 2–5% HNO_3, 1000 mg/L, VWR Chemicals), ethanol (C_2H_5OH, >99%, Carlo Erba), iron sulfate heptahydrate ($FeSO_4.7H_2O$, >99%, Merk), lithium chloride (LiCl, >99%, Sigma-Aldrich), methanol (HPLC grade, Fisher Scientific), nickel (Ni^{2+} in 5% HNO_3, 1000 mg/L, Alfa Aesar), nitric acid (HNO_3, puriss. p.a., 65%, Merck), N-methylimidazole (99%, Acros Organics), potassium hydroxide (KOH, >98%, Pronolab), potassium nitrate (KNO_3, >99%, Merk), sodium hydroxide (NaOH, >98%, Pronolab), and tetraethyl orthosilicate ($C_8H_{20}O_4Si$, TEOS, >99%, Sigma-Aldrich), toluene (99.8%, Fisher Scientific). The water used in the sorption experiments was double distilled, passed across a reverse osmosis system and further treated with a Milli-Q plus 185 water purification equipment.

Synthesis of Colloidal Magnetite (Fe_3O_4) Nanoparticles

Magnetic iron oxide NPs with an average size of 50 nm were synthesized by oxidative hydrolysis of iron sulphate in alkaline conditions, according to the procedure described in Oliveira-Silva et al.[23] (Scheme 1). Ultra-pure water was first deoxygenated with N_2 under vigorous stirring during 2 h. Then, 1.90 g (34 mmol) of KOH and 1.52 g (15 mmol) of KNO_3 were added to 25 mL of deoxygenated water using a 250 mL round flask. This mixture was heated at 60 °C, under N_2, and mechanically stirred at 500 rpm. After total dissolution, 25 mL of an aqueous solution of $FeSO_4.7H_2O$ (4.75 g, 17 mmol) was added dropwise to the mixture and mechanical stirring was increased to 700 rpm. The resulting

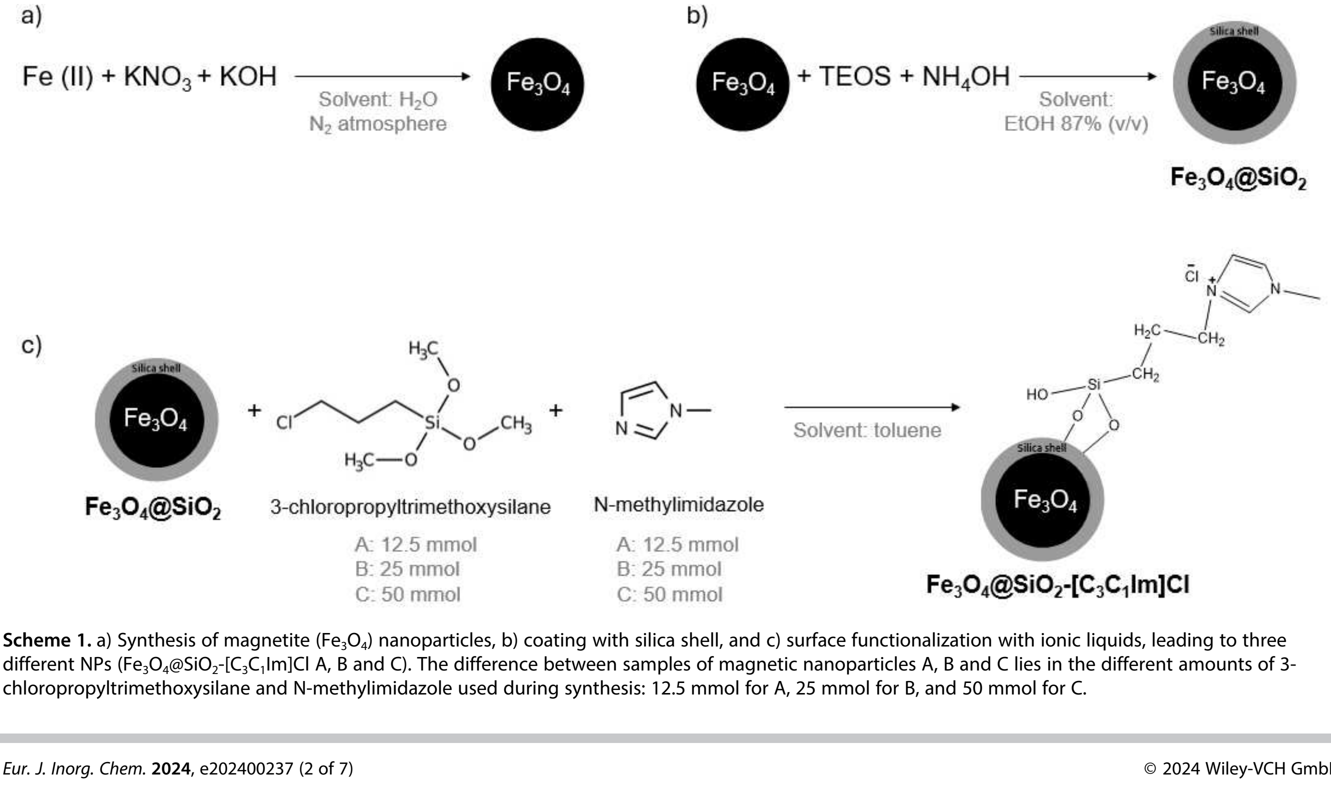

Scheme 1. a) Synthesis of magnetite (Fe_3O_4) nanoparticles, b) coating with silica shell, and c) surface functionalization with ionic liquids, leading to three different NPs ($Fe_3O_4@SiO_2$-$[C_3C_1Im]Cl$ A, B and C). The difference between samples of magnetic nanoparticles A, B and C lies in the different amounts of 3-chloropropyltrimethoxysilane and N-methylimidazole used during synthesis: 12.5 mmol for A, 25 mmol for B, and 50 mmol for C.

Research Article
doi.org/10.1002/ejic.202400237

solution presented a dark-green color after complete addition of the Fe(II) salt. The solution reacted for 30 min. After reaction, the round flask was transferred to an oil bath at 90 °C, keeping the reacting mixture under N_2 without stirring, during 4 h. Finally, the resulting black powder was collected and washed thoroughly with deoxygenated water and ethanol. After washing, the powder was dried in an oven set at 40 °C.

Coating of Magnetite Nanoparticles

The magnetite nanoparticles were modified at the surface using a sol-gel methods via the alkaline hydrolysis of TEOS to obtain core/shell Fe_3O_4@SiO_2 nanoparticles, according to the procedure described in Amiri et al.[24] (Scheme 1). Briefly, a dispersion of NPs (1.00 g) in a mixture of ethanol (80 mL) and ultra-pure water (20 mL) was prepared and left immersed in an ice bath, over 15 min under sonication (horn Sonics, Vibracell). Then, 2.15 mL of TEOS dissolved in ethanol (50 mL) and 6 mL of ammonia 25 % (v/v) were added and the suspension was left in an ice bath for more 10 min under sonication. Afterwards, the reaction proceeded at room temperature under continuous mechanic stirring at 600 rpm for 12 h. Finally, the silica-coated particles were washed with ultra-pure water and ethanol, collected using a permanent magnet and dried at room temperature.

Modification of Fe_3O_4@SiO_2 Nanoparticles with ILs

The modification of Fe_3O_4@SiO_2 nanoparticles with ILs was performed in a one-step reaction, based on the synthesis procedure previously reported by Amiri et al.[24] and Comès et al.[25] (Scheme 1). The Fe_3O_4@SiO_2 nanoparticles (1.5 g) were suspended in 100 mL of dried toluene, followed by the addition of 2.5 mL of 3-chloropropyltrimethoxysilane (12.5 mmol), and 1.0 mL of N-methylimidazole (12.5 mmol). This suspension was mechanically stirred at 700 rpm and refluxed for 24 h at 95 °C. After refluxing, the reaction was stopped, the NPs were collected using a magnet, and washed with toluene (50 mL), methanol (50 mL), water (50 mL), and again with methanol (25 mL). The obtained nanoparticles, Fe_3O_4@SiO_2-[C_3C_1Im]Cl A, were dried at 80 °C for 8 h prior to their characterization and sorption experiments. This procedure was repeated using twice and four times the amount of 3-chloropropyltrimethoxysilane and N-methylimidazole, obtaining the nanoparticles Fe_3O_4@SiO_2-[C_3C_1Im]Cl B and Fe_3O_4@SiO_2-[C_3C_1Im]Cl C, respectively. Thus, the difference between samples of magnetic nanoparticles Fe_3O_4@SiO_2-[C_3C_1Im]Cl A, B and C lies in the different amounts of 3-chloropropyltrimethoxysilane and N-methylimidazole used during synthesis: 12.5 mmol for A, 25 mmol for B, and 50 mmol for C.

Characterization Techniques

The chemical and physical characterization of the IL-supported magnetic nanoparticles was performed using various techniques. The crystalline phase in the powdered sample was identified by X-Ray diffraction (XRD) using an Empyrean PANalytical diffractometer (Cu $K_{\alpha1,2}$ X-radiation, $\lambda_1 = 1.54060$ Å; $\lambda_2 = 1.54443$ Å). The registration of the diffraction patterns was performed with a step size of 0.026 degrees, in continuous mode, in the $15 \leq 2\theta \leq 95°$ range. Fourier Transform Infrared (FTIR) spectra (in the range 4000–400 cm^{-1}) were recorded using a Bruker Tensor 27 spectrophotometer, equipped with an Attenuated Total Reflectance (ATR) accessory, after 256 scans with resolution of 4 cm^{-1}. The morphology of the NPs was analyzed by Transmission electron microscopy (TEM) (Electron Microscope JEOL, 2200FS, working at 200 kV, with resolution of 1 Å). Samples were prepared by direct deposition of an aliquot drop of an ethanolic suspension of particles over a grid of copper coated with a carbon film and then let to evaporate the solvent at room temperature. Elemental analysis for carbon, hydrogen and nitrogen contents (in weight percentage) was performed with a Truspec Micro CHNS 630–200-200 elemental analyzer, applying the following analysis parameters: sample of 2 mg; combustion furnace temperature of 1075 °C; afterburner temperature of 850 °C. Infrared absorption was used to determine the amount of carbon and hydrogen, and thermal conductivity was applied to determine the amount of nitrogen. The specific surface area (S_{BET}) of NPs was determined using an automated surface area analyzer (Quantachrome Autosorb IQ2) by means of nitrogen adsorption-desorption. Prior to the measurements, the samples were degassed overnight at 100 °C. Zeta potential measurements of the colloidal samples were performed using a Zetasizer Nano ZS (Malvern Instruments). The pH of the colloid was varied between 2 and 10, using NaOH or HNO_3 aqueous solutions. The temperature was kept at 25 °C, and three replicate measurements of zeta potential were performed for each sample. Measurements of hysteretic cycle to evaluate the magnetic properties of the NPs were performed using a SQUID magnetometer at 27 °C. The magnetization was normalized to the total mass of the sample.

Quantification of Lithium, Cobalt and Nickel

The quantification of lithium, cobalt and nickel was performed by Inductively Coupled Plasma-Optical Emission Spectrometry (ICP-OES), using a Horiba Jobin Yvon Activa M spectrometer (radial configuration) equipped with a Burgener MiraMist nebulizer (sample flow of 1 mL/min), peristaltic sample delivery pump with three canals, argon flow (nebulizer: 0.02 L/min; auxiliary gas: 0.2 L/min; plasma: 12 L/min), nebulizer chamber, CCD (coupled charging device) for detection, and algorithm background correction. Calibration curves were stablished using 5 standards with concentrations between 20 and 2000 μg/L, prepared by the dilution of Li, Co and Ni standard solutions into acidified water (1 % HNO_3 v/v). Only calibration curves with a correlation coefficient above 0.999 were considered. The limit of quantification was considered as the lowest concentration standard of the calibration curve (20 μg/L). The coefficient of variation between sample replicates (at least, three replicates were investigated) did not exceed 5 %.

Sorption Experiments

The ability of the Fe_3O_4@SiO_2-[C_3C_1Im]Cl (A, B and C) NPs to remove Li^+, Co^{2+} and Ni^{2+} from multielemental aqueous solution was evaluated by contacting 50 mg of NPs with an aqueous solution of Li, Co and Ni for 1 and 24 h. The sorption experiments were performed in batch mode, together with control assays, in Schott glass bottles of 100 mL at 25 °C, under stirring (250 rpm) and at different pH values. The solution of 2 mg/L of Li, Co and Ni was freshly prepared by dilution of the standard commercial solution (1000 mg/L) in ultra-pure water.

The influence of the pH of the solution and the influence of the bonding amount of the IL in the NPs surface in the removal of lithium, cobalt and nickel was investigated. The influence of pH was studied at pH values of 2, 4, 6, 8, 10 and 12 for an initial Li, Co and Ni concentration of 2 mg/L in ultra-pure water using 500 mg/L of Fe_3O_4@SiO_2-[C_3C_1Im]Cl B NPs. Adjustments of pH were performed HNO_3 or NaOH solutions. Fe_3O_4@SiO_2-[C_3C_1Im]Cl A and Fe_3O_4@SiO_2-[C_3C_1Im]Cl C NPs were applied for the removal of Li, Co and Ni from solutions at pH 10 to evaluate the effect on bonding amount of ILs in the NPs surface.

In all the experiments, the start time (t_0) was assumed the time that the sorbent was first mixed with the aqueous solution. NPs were placed in contact with spiked solution of the elements and after 1 and 24 h of contact, aliquots (5–10 mL) of sample were collected using a Pasteur pipette. These aliquots were under the influence of a magnet for approximately 5 min to ensure that all particles were removed. After separation of the particles, aliquots were immediately acidified (pH < 2) with 25 μL of concentrated HNO_3 (65% v/v) and stored at 4 °C until analysis by ICP-OES.

To evaluate the effectiveness of the sorption process, the removal percentages were determined using Equation (1). The variation of ion concentration along the contact time with the sorbent material are expressed in terms of normalized concentrations (Equation (2)), which allows the comparison of the removal efficiency by various sorbates for a given sorbent, or using the same sorbate but different sorbents, regardless of the initial sorbate concentration.

$$\text{Removal }(\%) = \frac{(C_0 - C_t)}{C_0} * 100 \tag{1}$$

$$C_t' = \frac{C_t}{C_0} \tag{2}$$

where C_0 is the initial concentration, C_t is the concentration in the liquid fraction at a certain time t, and C_t is the normalized concentration.

Results and Discussion

Characterization of the Prepared NPs

The powder XRD patterns of the several samples containing the magnetic NPs (Figure S1 in Supporting Information) showed the characteristic peaks for Fe_3O_4 (2θ = 18.3°, 30.1°, 35.5°, 43.1°, 53.5°, 57.0°, 62.6° and 89.7°) ascribed to the reflections (1 1 1), (2 2 0), (3 1 1), (4 0 0), (4 2 2), (5 1 1), (4 4 0) and (7 3 1) (JCPDS file No. 19-0629). Thus, the X-ray diffractograms confirm the presence of Fe_3O_4, used as the starting nanomaterial; subsequent coating and functionalization steps did not bring significant changes on the magnetite structure.

Figure 1 shows the FTIR-ATR spectra of Fe_3O_4, Fe_3O_4@SiO_2 and Fe_3O_4@SiO_2-[C_3C_1Im]Cl (A, B and C) that confirm the surface functionalization of the NPs using the selected ILs. The spectrum of Fe_3O_4 NPs displays a strong band at 540 cm^{-1}, which is attributed to the stretching vibrational mode of lattice Fe–O bond[26]. The coated particles' reveal in the FTIR spectrum a band around 1050 cm^{-1}, which corresponds to the asymmetric Si–O–Si stretching vibration mode of amorphous SiO_2. Additionally, the bands of the O–Si–O deformation mode of amorphous SiO_2 and the symmetric Si–O–Si stretching vibration are evident at 430 cm^{-1} and 790 cm^{-1}, respectively.[26] In the spectra of functionalized NPs, the diminishing of the band associated to the bending vibration absorption of Si–OH, observed at 935 cm^{-1} in the spectrum of Fe_3O_4@SiO_2, indicates the successful functionalization of silica.[27] The spectra of [Si][C_3C_1Im]Cl B and C also present a weak band at 1556 cm^{-1}, which is attributed to the frequency of the imidazole ring[27].

Figure 2 depicts the TEM images of Fe_3O_4, Fe_3O_4@SiO_2 and Fe_3O_4@SiO_2-[C_3C_1Im]Cl (A, B and C) NPs. These images show NPs of nearly spheroidal shape with an average diameter about 65 nm, with a thin coating layer of about 22 nm thickness for the samples surface modified with silica. Furthermore, no significant morphological differences were observed in the magnetic cores of the functionalized NPs as compared to the original magnetite particles.

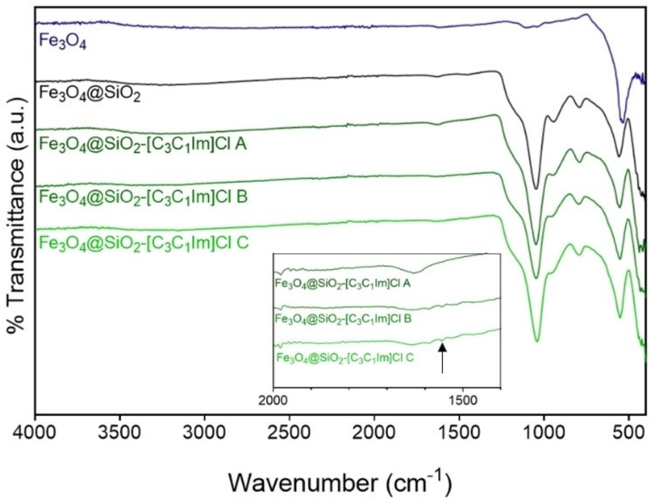

Figure 1. FTIR-ATR spectra of Fe_3O_4, Fe_3O_4@SiO_2 and Fe_3O_4@SiO_2-[C_3C_1Im]Cl (A, B and C) NPs.

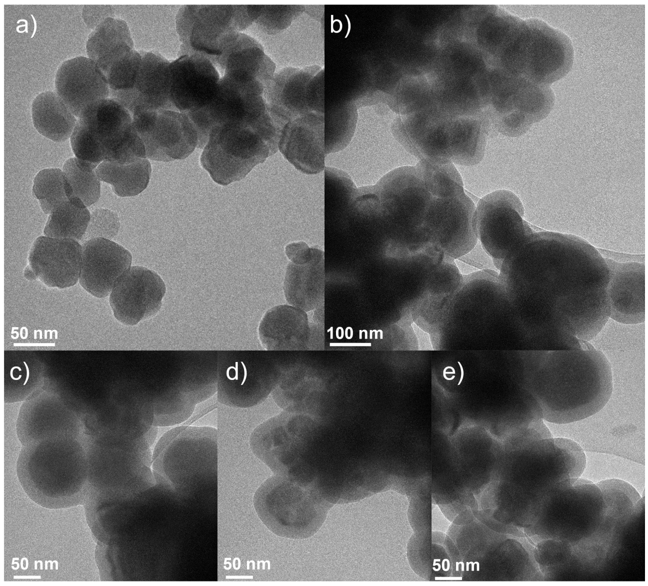

Figure 2. TEM images of: a) Fe_3O_4, b) Fe_3O_4@SiO_2, c) Fe_3O_4@SiO_2-[C_3C_1Im]Cl A, d) Fe_3O_4@SiO_2-[C_3C_1Im]Cl B and e) Fe_3O_4@SiO_2-[C_3C_1Im]Cl C NPs.

The successful functionalization of the NPs was additionally confirmed through elemental analysis. The carbon, hydrogen and nitrogen contents in the synthetic samples are indicated in Table 1. It should be noted that the vestigial amounts of carbon, hydrogen and nitrogen detected in Fe_3O_4 and Fe_3O_4@SiO_2 NPs result from the reagents used during the synthesis. The carbon and nitrogen contents (in weight fraction percentage) in functionalized NPs range from 0.460% to 1.986% and from 0.214% to 1.101%, respectively. These results confirm the functionalization of NPs Fe_3O_4@SiO_2-[C_3C_1Im]Cl B and C. Never-

Research Article
doi.org/10.1002/ejic.202400237

Table 1. Results of elemental analysis and values of BET surface area (S_{BET}), porosity volume (Vp) and pore diameter (Dp) of the NPs used in this work.

Nanoparticles	%C	%H	%N	Bonding amount (mmol/g)	S_{BET} (m^2/g)	V_p (cm^3/g)	D_p (nm)
Fe_3O_4	0.061	0.258	0.050	–	16.58	0.207	44.391
Fe_3O_4@SiO_2	0.447	1.029	0.396	–	12.79	0.068	3.114
Fe_3O_4@SiO_2-[C_3C_1Im]Cl A	0.460	0.624	0.214	0.076	11.61	0.078	3.114
Fe_3O_4@SiO_2-[C_3C_1Im]Cl B	1.959	0.791	1.101	0.393	14.54	0.096	3.108
Fe_3O_4@SiO_2-[C_3C_1Im]Cl C	1.986	0.813	1.039	0.371	16.54	0.109	3.111

theless, due to the low amount of IL groups in the NPs surface, the functionalization of NPs Fe_3O_4@SiO_2-[C_3C_1Im]Cl A can not be confirmed. On the other hand, there are no significant changes in the functionalization degree of Fe_3O_4@SiO_2-[C_3C_1Im]Cl B and Fe_3O_4@SiO_2-[C_3C_1Im]Cl C NPs. This suggests that the stoichiometric amount of 3-chloropropyltrimethoxysilane and N-methylimidazole (25 mmol) employed in the functionalization allows an extensive surface functionalization.

The specific surface area of the synthesized NPs was determined by nitrogen adsorption using the BET (Brunauer-Emmett-Teller) method, whose results are given in Table 1. A decrease of the specific surface area of Fe_3O_4@SiO_2 is observed when compared to the uncoated magnetite particles. Moreover, it increases as the amount of precursors used in the functionalization of IL-modified NPs had increased. Silica has the highest value of pore diameter (44.391 nm), and the IL-modified NPs show a pore diameter between 3.108 and 3.114 nm.

The bonding amount of ILs onto NPs was determined from the elemental analysis data. In these calculations, the percentage amount of nitrogen was employed, taking into account that each molecule of methylimidazole has 2 nitrogen atoms. The higher number of IL functional groups appears in the Fe_3O_4@SiO_2-[C_3C_1Im]Cl B NPs, followed by Fe_3O_4@SiO_2-[C_3C_1Im]Cl C and Fe_3O_4@SiO_2-[C_3C_1Im]Cl A, with values decreasing from 0.393 to 0.076 mmol/g. As will be discussed later, these values are relevant for interpreting the materials' performance in sorbing lithium, cobalt and nickel.

Zeta potential measurements were performed to determine the point of zero charge (PZC) of the functionalized colloidal NPs, which is the pH value at which a solid particle in suspension exhibits zero net electrical charge on its surface. Figure 3 displays zeta potentials as a function of solution pH for Fe_3O_4@SiO_2, Fe_3O_4@SiO_2-[C_3C_1Im]Cl A, Fe_3O_4@SiO_2-[C_3C_1Im]Cl B and Fe_3O_4@SiO_2-[C_3C_1Im]Cl C NPs. At pH 2.59, 8.97, 8.89 and 6.52, the net charge of Fe_3O_4@SiO_2, Fe_3O_4@SiO_2-[C_3C_1Im]Cl A, Fe_3O_4@SiO_2-[C_3C_1Im]Cl B and Fe_3O_4@SiO_2-[C_3C_1Im]Cl C NPs is zero. All functionalized NPs display higher PZC values as compared to Fe_3O_4@SiO_2, confirming the presence of a cation in NPs and the successful silica functionalization. In addition, despite the functionalization of Fe_3O_4@SiO_2-[C_3C_1Im]Cl A NPs not being detected through elemental analysis results, their PZC value of 8.97 proved that the ILs were successfully covalently attached to the silica surface.

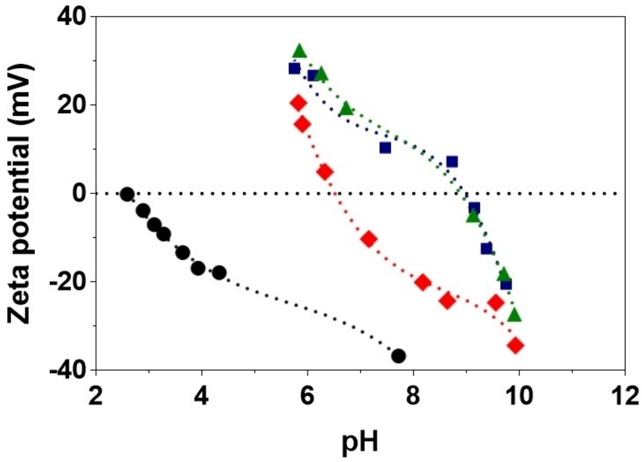

Figure 3. Zeta potentials as a function of solution pH for (●) Fe_3O_4@SiO_2, (■) Fe_3O_4@SiO_2-[C_3C_1Im]Cl A, (▲) Fe_3O_4@SiO_2-[C_3C_1Im]Cl B and (♦) Fe_3O_4@SiO_2-[C_3C_1Im]Cl C NPs.

The magnetic measurements performed for the samples Fe_3O_4, Fe_3O_4@SiO_2, Fe_3O_4@SiO_2-[C_3C_1Im]Cl B are shown in Figure S2 (in Supporting Information). These samples show magnetic hysteresis as expected for ferrimagnetic magnetite particles with the dimensions as discussed above.

Coercivity (H_C), remanent magnetization (M_R) and saturation magnetization (M_S) values obtained from the magnetization cycles are provided in Table 2. The saturation magnetization for magnetite NPs, around 80 emu/g at 27 °C, is within the reported values for this material.[23,28] Also, this value is very close to the value for bulk magnetite (92 emu/g).

The modified nanoparticles (Fe_3O_4@SiO_2 and Fe_3O_4@SiO_2-[C_3C_1Im]Cl B) show lower values of saturation magnetization than the uncoated magnetite NPs, due to the diamagnetic coating material. Still, the observed saturation magnetization for the surface modified samples is high (42 and 51 emu/g, respectively).

Table 2. Magnetic parameters for magnetite, Fe_3O_4@SiO_2 and Fe_3O_4@SiO_2-[C_3C_1Im]Cl B samples.

Sample	$M_S \pm \Delta$ (emu/g)	$H_C \pm \Delta$ (Oe)	$M_R \pm \Delta$ (emu/g)
Fe_3O_4	81 ± 1	102 ± 11	10.4 ± 0.4
Fe_3O_4@SiO_2	42 ± 1	93 ± 7	4.2 ± 0.1
Fe_3O_4@SiO_2-[C_3C_1Im]Cl B	51 ± 1	93 ± 7	5.3 ± 0.1

Regarding the coercivity, all the samples present similar values, which is consistent with magnetite cores with preserved magnetic properties after silica encapsulation and surface functionalization.

Sorption Experiments of Lithium, Cobalt and Nickel in Fe_3O_4@SiO_2-[C_3C_1Im]Cl NPs

The ability of the synthesized NPs to separate Li, Co and Ni from multielemental aqueous solution was evaluated by performing sorption experiments of batch (discontinuous) type. In these experiments, the influence of the pH of the solution and the effect of the bonding amount of ILs in the NPs surface in the sorption process were evaluated. The sorption of Li, Co and Ni on Fe_3O_4@SiO_2-[C_3C_1Im]Cl B NPs, after 1 h, was evaluated at pH 2, 4, 6, 8, 10 and 12. The results obtained are depicted in Figure 4.

The sorption only occurs for Co and Ni, and at alkaline pH values (pH 10 and 12), which aligns well with the conditions of the leaching process. Spent LIB powders have been leached using ammonia due to the selective leaching ammonia characteristics between the desired metals (Li, Ni, Co) and undesired metals (Al and Mn). Also, transition metal cations of Co and Ni form stable complexes with NH_3, making ammonia leaching thermodynamically feasible. Based on this, Wang et al.[4] used ammonia – ammonium hydrocarbonate ($NH_3 \cdot H_2O$ – NH_4HCO_3) solutions in the presence of hydrogen peroxide (H_2O_2) to leach the pre-treated spent LIB powders. The authors obtained a leaching solution containing Li, Ni, Co, and ammonia ions, which was further used in a sorption separation step. The NPs developed in this work could be applied in this step to separate cobalt and nickel from lithium, obtaining a lithium containing alkaline solution. Moreover, the sorption of cobalt and nickel at surface sites, in the conditions studied, is fast (1 h).

Based on Pourbaix diagrams,[29] the alkalization of the solution at pH 10 and 12 can result in $Co(OH)_2$ and $Ni(OH)_2$ precipitates. However, as shown in Figure 5, the analysis of the controls (i.e. metals solution without the addition of NPs) indicates that 1 h is not enough to precipitation to occur. For longer periods of contact, both cobalt and nickel species start to precipitate at pH 12.

Since the controls are stable at pH 10 and no precipitation of cobalt and nickel was observed for short periods of contact time, the effect of the ILs amount on the NPs surface was evaluated on a multielemental solution of Li, Co and Ni for 1 h of contact between the NPs and the metals, as shown in Figure 6.

The results obtained show that Fe_3O_4@SiO_2-[C_3C_1Im]Cl B NPs were those with high efficiency for Co and Ni, achieving 99% of recovery for both elements. Moreover, comparing Fe_3O_4@SiO_2-[C_3C_1Im]Cl B and Fe_3O_4@SiO_2-[C_3C_1Im]Cl C NPs, the bonding amount of IL on NPs surface does not increase with the use of more reagents amount during the synthesis, concluding that a proportion of 25 mmol of both cation and anion is the ideal amount for the functionalization of NPs.

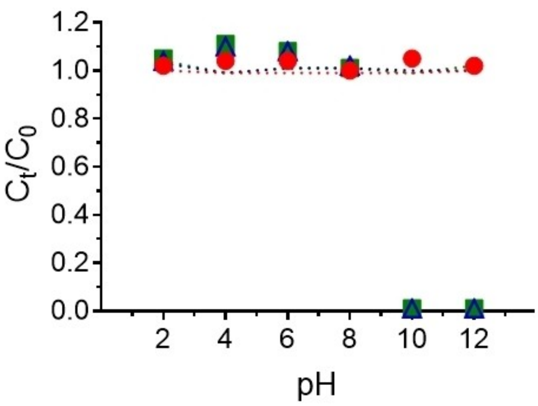

Figure 4. Sorption efficiency of Fe_3O_4@SiO_2-[C_3C_1Im]Cl B with: ● lithium (— control), Δ cobalt (— control) and ■ nickel (— control), at different pH values. Multielemental solution of 2 mg/L Li, Co and Ni, pH 2–12, 500 mg MSIL/L, 60 min of sorption.

Conclusions

In this study, we synthesized, characterized, and assessed ionic-liquid-supported magnetic nanoparticles as sorption materials to separate cobalt and nickel species from lithium dissolved in aqueous solutions. The magnetic nanosorbents were prepared by covalently attaching the IL cation to the surface of silica-coated magnetite NPs, using imidazolium as the cation and chloride as the counter-ion.

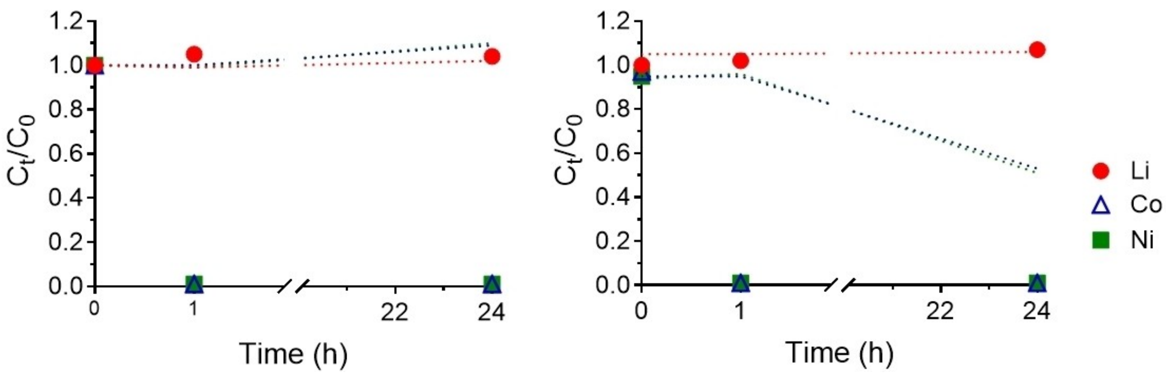

Figure 5. Sorption efficiency of Fe_3O_4@SiO_2-[C_3C_1Im]Cl B with: ● lithium (— control), Δ cobalt (— control) and ■ nickel (— control), after 1 and 24 h of sorption. Multielemental solution of 2 mg/L Li, Co and Ni, pH 10 (on left) and pH 12 (on right), 500 mg MSIL/L.

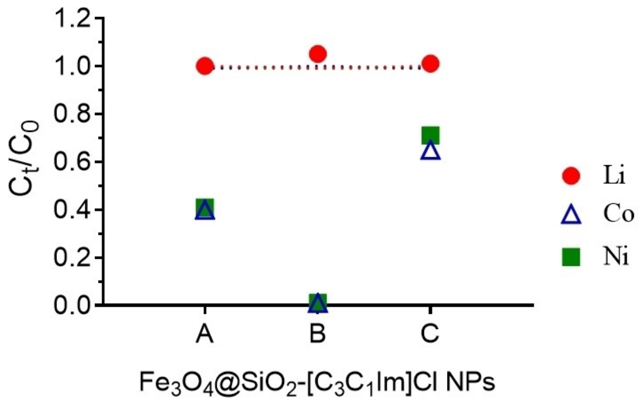

Figure 6. Sorption efficiency of the three magnetic SILs with: ● lithium (— control), △ cobalt (— control) and ■ nickel (— control). Multielemental solution of 2 mg/L Li, Co and Ni, pH 10, 500 mg MSIL/L, 60 min sorption.

Different degrees of functionalization were studied, with a proportion of 25 mmol of both cation and anion found to achieve the maximum degree of functionalization. The sorption performance was assessed at various pH values, confirming that alkaline conditions (specifically pH 10 and 12) are necessary for the metals to form anionic complexes, thereby enhancing their sorption onto the IL-modified NPs. Furthermore, the sorption of cobalt and nickel at surface sites, under the studied conditions, occurs rapidly (within 1 hour).

Considering the research on the use of SILs for metal recovery, this work introduces the use of IL-supported magnetic nanoparticles for the magnetic separation of Co^{2+} and Ni^{2+} from Li^{+}. Overall, the application of IL-modified magnetic NPs resulted in good performances for the separation of Co^{2+} and Ni^{2+} from Li^{+} and should be applied on lixiviates of spent LIB as a sorbent material.

Acknowledgments

The authors acknowledge the financial support to LAQV-REQUIMTE [within the scope of the projects UIDB/50006/2020 & UIDP/50006/2020], financed by national funds through the FCT/MCTES. This work was developed within the scope of the project CICECO - Aveiro Institute of Materials, UIDB/50011/2020 (DOI 10.54499/UIDB/50011/2020), UIDP/50011/2020 (DOI 10.54499/UIDP/50011/2020) & LA/P/0006/2020 (DOI 10.54499/LA/P/0006/2020), financed by national funds through the FCT/MCTES (PIDDAC). Joana C. Almeida and Celso E. D. Cardoso thank FCT/MCTES (Fundação para a Ciência e Tecnologia and Ministério da Ciência, Tecnologia e Ensino Superior) and ESF (European Social Fund) through NORTE 2020 (Programa Operacional Região Norte) for the PhD grants SFRH/BD/139471/2018 and 2021.06684.BD, respectively.

Conflict of Interests

The authors declare no conflict of interest.

Data Availability Statement

Data sharing is not applicable to this article as no new data were created or analyzed in this study.

Keywords: Cobalt · Ionic liquids · Magnetic nanoparticles · Nickel · Sorption

[1] B. Scrosati, J. Garche, *J. Power Sources* **2010**, *195*, 2419–2430.
[2] European Commission, *Report on Critical Raw Materials and the Circular Economy*, **2018**.
[3] B. Swain, *Sep. Purif. Technol.* **2017**, *172*, 388–403.
[4] H. Wang, K. Huang, Y. Zhang, X. Chen, W. Jin, S. Zheng, Y. Zhang, P. Li, *ACS Sustain. Chem. Eng.* **2017**, *5*, 11489–11495.
[5] T. Fernandes, S. Soares, T. Trindade, A. Daniel-da-Silva, *Nanomaterials* **2017**, *7*, 68.
[6] S. F. Soares, T. Fernandes, T. Trindade, A. L. Daniel-da-Silva, *Environ. Chem. Lett.* **2019**, 1–14.
[7] F. Šulek, M. Drofenik, M. Habulin, Ž. Knez, *J. Magn. Magn. Mater.* **2010**, *322*, 179–185.
[8] S. F. Soares, T. Fernandes, M. Sacramento, T. Trindade, A. L. Daniel-da-Silva, *Carbohydr. Polym.* **2019**, *203*, 35–44.
[9] Z. Lei, B. Chen, Y. M. Koo, D. R. Macfarlane, *Chem. Rev.* **2017**, *117*, 6633–6635.
[10] S. P. M. Ventura, F. A. e Silva, M. V. Quental, D. Mondal, M. G. Freire, J. A. P. Coutinho, *Chem. Rev.* **2017**, *117*, 6984–7052.
[11] P. A. Yudaev, E. M. Chistyakov, *ChemEngineering* **2022**, *6*, 1–22.
[12] R. Chen, *J. Ion. Liq.* **2023**, *3*, 100070.
[13] N. Schaeffer, H. Passos, M. Gras, S. J. Rodriguez Vargas, M. C. Neves, L. Svecova, N. Papaiconomou, J. A. P. Coutinho, *ACS Sustain. Chem. Eng.* **2020**, *8*, 12260–12269.
[14] E. A. Othman, A. G. J. van der Ham, H. Miedema, S. R. A. Kersten, *Sep. Purif. Technol.* **2020**, *252*, 117435.
[15] A. Q. Pedro, J. A. P. Coutinho, M. G. Freire, *in Encycl. Ion. Liq.*, Springer, Singapore **2019**, 1–12.
[16] G. Zante, M. Boltoeva, A. Masmoudi, R. Barillon, D. Trébouet, *Sep. Purif. Technol.* **2020**, *252*, 117477.
[17] J. Gega, W. Walkowiak, B. Gajda, *Sep. Purif. Technol.* **2001**, *22–23*, 551–558.
[18] N. E. Belkhouche, M. A. Didi, R. Romero, J. Å. Jönsson, D. Villemin, *J. Memb. Sci.* **2006**, *284*, 398–405.
[19] G. Zante, M. Boltoeva, A. Masmoudi, R. Barillon, D. Trébouet, *J. Memb. Sci.* **2019**, *580*, 62–76.
[20] F. Shojaeipoor, D. Elhamifar, R. Moshkelgosha, B. Masoumia, *J. Taiwan Inst. Chem. Eng.* **2016**, *67*, 166–173.
[21] A. V. Panteleimonov, M. O. Onizhuk, I. V. Khristenko, I. I. Chuiko, O. S. Tkachenko, Y. Gushikem, Y. V. Kholin, *J. Braz. Chem. Soc.* **2015**, *26*, 1160–1170.
[22] R. Hanzel, P. Rajec, *J. Radioanal. Nucl. Chem.* **2000**, *246*, 607–615.
[23] R. Oliveira-Silva, J. Pinto da Costa, R. Vitorino, A. L. Daniel-da-Silva, *J. Mater. Chem. B* **2015**, *3*, 238–249.
[24] M. Amiri, Yadollah Yamini, M. Safari, H. Asiabi, *Microchim. Acta* **2016**, *183*, 2297–2305.
[25] A. Comès, X. Collard, L. Fusaro, L. Atzori, M. G. Cutrufello, C. Aprile, *RSC Adv.* **2018**, *8*, 25342–25350.
[26] S. F. Soares, T. R. Simões, M. António, T. Trindade, A. L. Daniel-da-Silva, *Chem. Eng. J.* **2016**, *302*, 560–569.
[27] S. C. Bernardo, B. R. Araújo, A. C. A. Sousa, R. A. Barros, A. C. Cristovão, M. C. Neves, M. G. Freire, *Eur. J. Inorg. Chem.* **2020**, *2020*, 2380–2389.
[28] P. I. Girginova, A. L. Daniel-da-Silva, C. B. Lopes, P. Figueira, M. Otero, V. S. Amaral, E. Pereira, T. Trindade, *J. Colloid Interface Sci.* **2010**, *345*, 234–240.
[29] N. Takeno, *Atlas of Eh-PH Diagrams: Intercomparison of Thermodynamic Databases* **2005**.

Manuscript received: April 26, 2024
Revised manuscript received: July 4, 2024
Accepted manuscript online: July 4, 2024
Version of record online: ■■, ■■

RESEARCH ARTICLE

Explore the innovative use of ionic-liquid (IL) functionalized magnetic nanoparticles (NPs) for efficient recovery of cobalt (Co) and nickel (Ni) from aqueous containing these metals. This research highlights the potential of magnetic NPs in addressing the challenges of sustainable recycling in the context of the circular economy.

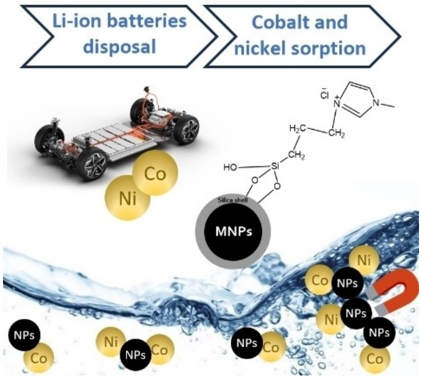

*J. C. Almeida, C. E. D. Cardoso, M. Neves, T. Trindade, M. G. Freire, E. Pereira**

1 – 8

Ionic-Liquid-Supported Magnetic Nanoparticles: Synthesis, Characterization, and Their Use for the Separation of Co and Ni from Li in Aqueous Solutions